PROPAGATION OF GUIDED ELASTIC WAVES IN ORTHOTROPIC PLATES

Y. Li and R. B. Thompson

Department of Engineering Science and Mechanics
Ames Laboratory
Iowa State University
Ames, Iowa 50011

INTRODUCTION

Numerical studies of wave propagation in free anisotropic plates were conducted at Stanford University in the early 70's [1,2], followed by a flurry of related work. Yet, this subject has not been completely understood. Recent years, however, have seen greatly increased interests in the influence of the anisotropy of composites and textured metal plates on Lamb wave propagation characteristics. This paper presents the basic theory for the propagation of guided elastic waves in orthotropic plates. Included are both numerical results and analytical or semianalytical expressions for the generalized Rayleigh-Lamb dispersion equations. As examples, comparisons are made of the dispersion curves for isotropic, weakly orthotropic, and strongly orthotropic plates with emphasis on the behavior of the zeroth order symmetric, antisymmetric, and horizontally polarized sheer modes.

DEVELOPMENT OF DISPERSION EQUATIONS

The method employed here for analysis of wave propagation in an anisotropic free plate is the so called "superposition of partial waves" [1,2,4], where the final solutions for displacement are obtained through summation of all possible partial plane waves. Let us consider a free plate having orthotropic symmetry with Cartesian coordinates axes coinciding with the three symmetry axes as shown in Fig. 1. For a general elastic, homogeneous and orthotropic medium, the Christoffel equations for plane waves are

$$\begin{bmatrix} A_{11} & A_{12} & A_{13} \\ A_{12} & A_{22} & A_{23} \\ A_{13} & A_{23} & A_{33} \end{bmatrix} \tag{1}$$

where

$$\begin{aligned} A_{11} &= C_{11}k_1^2 + C_{66}k_2^2 + C_{55}k_3^2 - \rho\omega^2 \\ A_{22} &= C_{66}k_1^2 + C_{22}k_2^2 + C_{44}k_3^2 - \rho\omega^2 \\ A_{33} &= C_{55}k_1^2 + C_{44}k_2^2 + C_{33}k_3^2 - \rho\omega^2 \\ A_{23} &= (C_{23} + C_{44})k_2k_3 \\ A_{13} &= (C_{13} + C_{55})k_1k_3 \\ A_{12} &= (C_{12} + C_{66})k_1k_2 \end{aligned} \tag{1'}$$

In equations (1'), k_i are the wave numbers in X_i directions, and n_i are the components of eigenvectors in X_i directions. To obtain the plate wave solutions consider the superposition of all plane wave solutions sharing common values of frequency ω and wave number k as illustrated in Fig. 2.

Examination of Eq. (1) shows that there will be three pairs of eigenvalues for k_3, leading to six plane wave solutions (eigenvectors). To determine the relative magnitudes of these six partial plane waves, stress free boundary conditions must be satisfied by the superposition on both the top and bottom surfaces of the plate; i.e. $\sigma_{13}=\sigma_{23}=\sigma_{33}=0$ at $X_3=\pm b/2$. Imposing these boundary conditions leads to a set of six linear homogeneous equations for U_p, the relative magnitudes of partial plane waves. Because of the characteristics of the three pairs of eigenvalues for k_3 and the fact that the X_1-X_2 plane exhibits mirror symmetry, plate wave solutions can be classified into two groups: antisymmetric and symmetric solutions according to the symmetry of the displacement field with respect to the central plane of the plate. Simple relations between the magnitudes of each pair of partial plane waves whose k_3^2 are identical follow, reducing the six linear equations for U_p to a pair of three linear equations. For nontrivial solutions, the determinant of the coefficient matrix of these linear equations must vanish, giving rise to the dispersion equations $f(\omega,k)=0$, where $k=\sqrt{k_1^2+k_2^2}$ is the wave number in propagation direction α.

We have developed analytical or semi-analytical expressions for the function $f(\omega,k)$. When the wave propagates in the direction α with respect to the X_1 direction, the dispersion equations are

$$P_1\left[\tan\left(\frac{\pi}{2}\sqrt{R_1}\right)\right]^{\pm 1}+P_2\left[\tan\left(\frac{\pi}{2}\sqrt{R_2}\right)\right]^{\pm 1}+P_3\left[\tan\left(\frac{\pi}{2}\sqrt{R_3}\right)\right]^{\pm 1}=0 \qquad (2)$$

where

$$P_1=P(R_1,R_2,R_3),\quad P_2=P(R_2,R_3,R_1),\quad P_3=P(R_3,R_1,R_2),$$

$$P(X,Y,Z)=\sqrt{X}[C_{13}K_1N_x(X)+C_{23}K_2N_y(X)+C_{33}N_z(X)]\cdot$$
$$\{[YN_x(Y)+N_z(Y)][ZN_y(Z)+N_z(Z)]-[YN_y(Y)+N_z(Y)][ZN_x(Z)+N_z(Z)]\}$$

$$N_x(X)=(C_{23}+C_{44})(C_{12}+C_{66})K_2-(C_{13}+C_{55})(C_{66}K_1+C_{22}K_2+C_{44}X-C_{66}W)$$

$$N_y(X)=(C_{13}+C_{55})(C_{12}+C_{66})K_1-(C_{23}+C_{44})(C_{11}K_1+C_{66}K_2+C_{55}X-C_{66}W)$$

$$N_z(X)=(C_{66}K_1+C_{22}K_2+C_{44}X-C_{66}W)(C_{11}K_1+C_{66}K_2+C_{55}X_3-C_{66}W)-$$
$$(C_{12}-C_{66})^2K_1K_2$$

$$K_1=K\cos^2\alpha,\qquad K_2=K\sin^2\alpha,\qquad K=\left(\frac{b}{\pi}k\right)^2,\qquad W=\frac{\rho\omega^2}{C_{66}}\left(\frac{b}{\pi}\right)^2$$

and $R_i=\left(\frac{b}{\pi}r_i\right)^2$, are the three eigenvalues for k_3^2 of Eq. (1).

In Eq. (2), the "-" exponent is for symmetric solutions and the "+" exponent is for antisymmetric solutions. In general, there are infinite number of possible roots for ω for a given wave number k, just as for waves propagating in an isotropic free plate. When the wave propagation

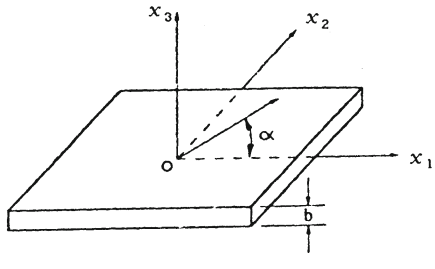

Fig. 1. Coordinates of a free orthotropic plate.

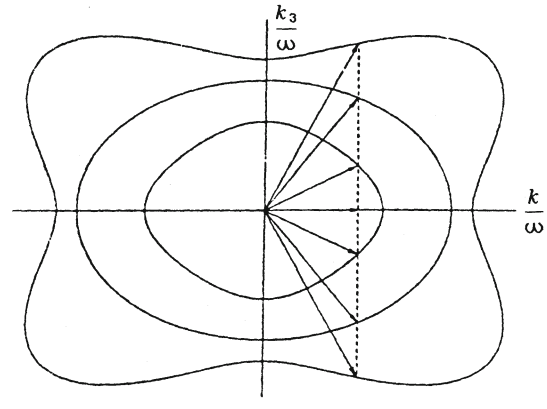

Fig. 2. Partial wave slownesses for a fixed ω and k $(k=\sqrt{k_1^2+k_2^2})$.

direction coincides with a symmetry axis, there are always partial waves whose polarization directions lie on the plane of the plate. Since these two SH (horizontal shear) waves decoupled from the other partial waves, further simplifications can be made to Eq. (2). If the wave propagation direction is in X_1 direction, the resulting dispersion equations for SH waves are:

$$\left[\tan\left(\frac{\pi}{2}\sqrt{R_1}\right)\right]^{\pm 1} = 0, \qquad R_1 = \frac{C_{66}}{C_{44}}(W-K) \tag{3}$$

or, explicitly,

$$\frac{C_{66}}{C_{44}}(W-K) = n^2, \qquad \text{n--nonnegative integer} \tag{3'}$$

In Eq. (3), "-" is for symmetric modes and "+" is for antisymmetric modes. In Eq. (3'), the solutions are symmetric (or antisymmetric) when n is even (or odd).

The Rayleigh-Lamb waves, made up of partial waves polarized in the orthogonal (sagittal) plane, have the following dispersion expressions

$$Q_1\left[\tan\left(\frac{\pi}{2}\sqrt{R_2}\right)\right]^{\pm 1} - Q_2\left[\tan\left(\frac{\pi}{2}\sqrt{R_3}\right)\right]^{\pm 1} = 0 \tag{4}$$

where $Q_1 = Q(R_2, R_3)$, $\quad Q_2 = Q(R_3, R_2)$

$$Q(X,Y) = \sqrt{Y}(C_{13}X - C_{11}K + C_{66}W)[C_{33}C_{55}Y + (C_{11}C_{33} - C_{13}C_{55} - C_{13}^2)K - C_{33}C_{66}W] \tag{4a}$$

or $$Q(X,Y) = \sqrt{X}(C_{33}X - C_{13}K - C_{66}W)(C_{33}C_{55}Y - C_{13}C_{55}K + C_{13}C_{66}W) \tag{4b}$$

and R_2 and R_3 are roots of the following equations for K_3:

$$(C_{11}K + C_{55}K_3 - C_{66}W)(C_{55}K + C_{33}K_3 - C_{66}W) - (C_{13} + C_{55})^2 K K_3 = 0$$

The form of Eq. (4b) was independently derived by Markus, et al. [3]. When the definition (4a) for Q(X,Y) is used, the "-" exponent in Eq. (4) corresponds to symmetric modes and the "+" exponent corresponds to antisymmetric modes. When the definition (4b) for Q(X,Y) is used, the "-" and "+" exponents correspond to antisymmetric and symmetric modes respectively. Equation (4) can be further expressed as

$$\frac{\tan\left(\frac{\pi}{2}\sqrt{R_2}\right)}{\tan\left(\frac{\pi}{2}\sqrt{R_3}\right)} = \left(\frac{Q_2}{Q_1}\right)^{\pm 1} \tag{4c}$$

which resembles and, for an isotropic plate, reduces to the well known Rayleigh-Lamb wave dispersion equations [4].

If the wave propagates in X_2 direction, the following changes must be made to Eqs. (3) and (4): $C_{11} \to C_{22}$, $C_{13} \to C_{23}$, $C_{44} \to C_{55}$, $C_{55} \to C_{44}$.

DISPERSION CURVES AND ASSOCIATED FULL PLANE SLOWNESS CURVES

To illustrate the dispersion behavior of orthotropic free plates with different degrees of anisotropy, six sets of dispersion curves and their associated slowness curves are presented here in Figs. 3 and 4. The latter are included since they graphically illustrate the solutions of Christoffel's equation, which must be satisfied by the partial waves. The elastic constants for these plots are supplied in Table 1. Each of these may be thought of as a copper polycrystal, with the degree of anisotropy controlled by texture parameters.

Table 1. Elastic constants (in GPa)

Fig. 3	C_{11}	C_{22}	C_{33}	C_{23}	C_{13}	C_{12}	C_{44}	C_{55}	C_{66}
(a)	201	201	201	106	106	106	47.3	47.3	47.3
(b)	200	197	198	109	106	107	50.1	47.1	48.3
(c), (d)	170	150	163	135	115	128	76.1	56.2	68.9
(e), (f)	205	175	138	153	123	85.1	93.7	63.9	26.3

DISCUSSIONS AND CONCLUSIONS

Comparing the dispersion curves for anisotropic plates to that of an isotropic one, we note the following similarities and differences: In an isotropic plate, the SH waves are always decoupled from Rayleigh-Lamb waves, which are a superposition of SV and P partial waves. The SH wave slowness curve is identical to (overlaps) the SV wave slowness curve. In anisotropic plates, partial waves do not generally have "pure" polarizations which are either parallel or perpendicular to the propagation direction. SH waves become decoupled only when the propagation direction is also a symmetry direction. In orthotropic media, there are two such symmetry directions; in cubic media, there are four such symmetry directions.

For an isotropic plate, the dispersion curves and associated slowness curves can be divided into three distinct regions, each having different characters in the eigenvalues (or R_l) of Christoffel Eq. (1). Other than the fact that the SH and SV slowness curves overlap, there is no crossing among slowness curves. Since these regions control various features of dispersion curves, we have examined their character in anisotropic plates and observed up to seven regions for wave propagating in a general direction. When SH waves are decoupled, SH wave slowness and dispersion curves may cross curves associated with other polarizations. Furthermore, there may be regions where eigenvalues of Christoffel equation becomes complex. Table 2 lists the region characteristics for the given examples.

In isotropic dispersion curves, the S_0 and A_0 modes approach Rayleigh velocity monotonically as $bk \to \infty$, and the Rayleigh wave speed is always less than the lowest order SH wave speed. This may not be true for anisotropic plates [1,2,5]. Consider first propagation in symmetry direction x, for which SH waves are decoupled from Rayleigh-Lamb wave, it can be shown that Rayleigh wave velocity is a solution to Eq. (5),

$$A_3 Z^3 + A_2 Z^2 + A_1 Z + A_0 = 0 \tag{5}$$

where $Z = \rho V_R^2$, $A_3 = C_{33}(C_{55} - C_{33})$

$$A_2 = C_{33}[C_{55}(C_{33} - C_{11}) + 2(C_{11}C_{33} - C_{13}^2)]$$

$$A_1 = -(C_{11}C_{33} - C_{13}^2)(2C_{33}C_{55} + C_{11}C_{33} - C_{13}^2)$$

$$A_0 = C_{55}(C_{11}C_{33} - C_{13}^2)^2.$$

When the anisotropy is not very strong, as shown in Fig. 3 (b), the S_0 and A_0 modes still asymptotically approach the Rayleigh velocity monotonically, and the Rayleigh wave speed is less than SH_0 wave. When the anisotropy becomes strong, as in Fig. 3 (c) and 3 (e), the S_0 and A_0 modes approach the Rayleigh velocity in an oscillatory manner. The reason is that, in Fig. 3 (b), the Rayleigh velocity occurs in the region where all eigenvalues (excluding SH waves, of course) are imaginary, while in Figs. 3 (c) and 3 (e), Rayleigh velocity falls in the region where all eigenvalues are complex.

Table 2. Region Characteristics for Eigenvalues.

Fig. 3	A	B	C	D	E	F	Total
(a)	1	1	0	0	0	1	3
(b)	1	1	1	0	1	1	5
(c)	1	2	1	0	1	0	5
(d)	1	2	1	0	1	0	5
(e)	2	1	0	1	1	0	5
(f)	3	1	0	2	1	0	7

A: All eigenvalues are real;
B: One pair is pure imaginary, the other two pairs are real;
C: Two pairs are pure imaginary, the other pair is real;
D: One pair is real, the other two pairs are complex conjugates;
E: One pair is pure imaginary, the other two pairs are complex conjugates.
F: All eigenvalues are imaginary.

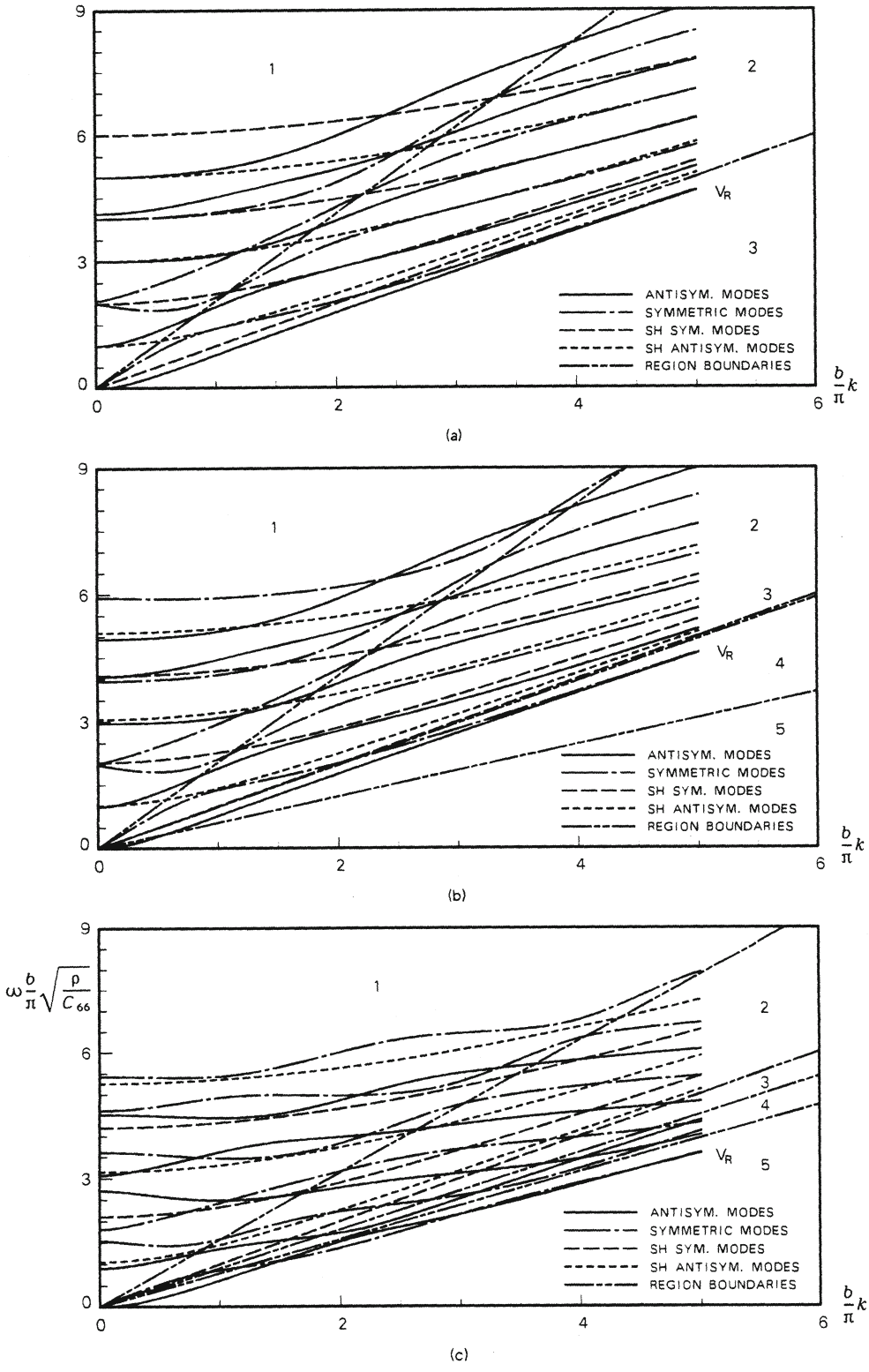

Fig. 3. Dispersion curves for orthotropic free plates with different anisotropy and propagation angle α. (a) Isotropic; (b) Weakly orthotropic (α = 0); (c) Strongly orthotropic (α = 0);

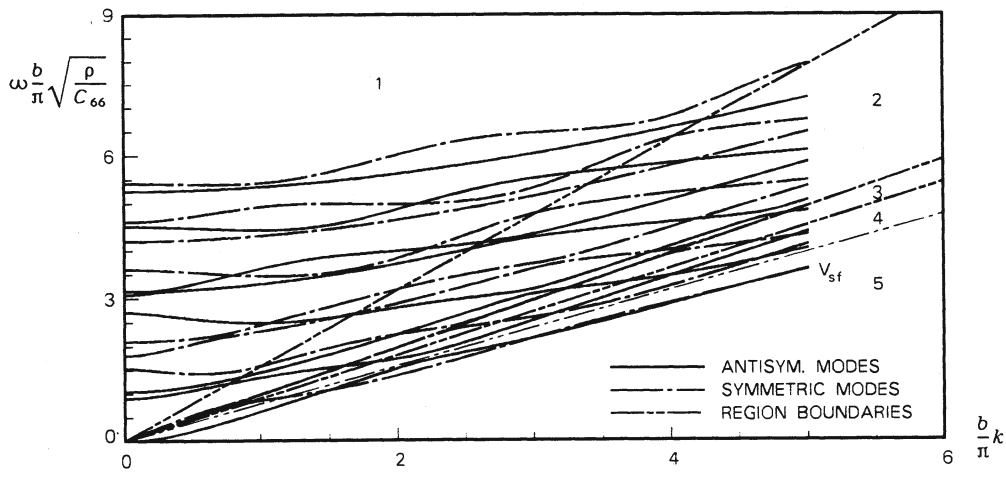

(d)

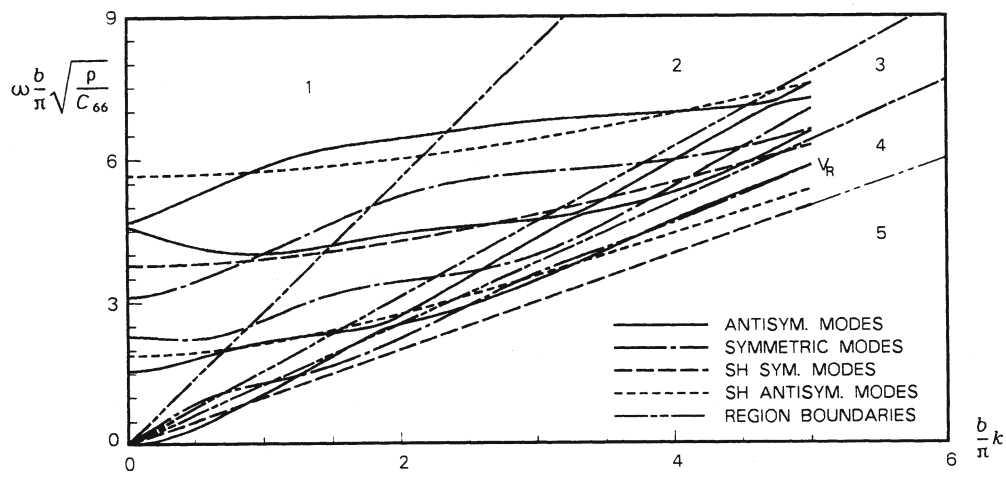

(e)

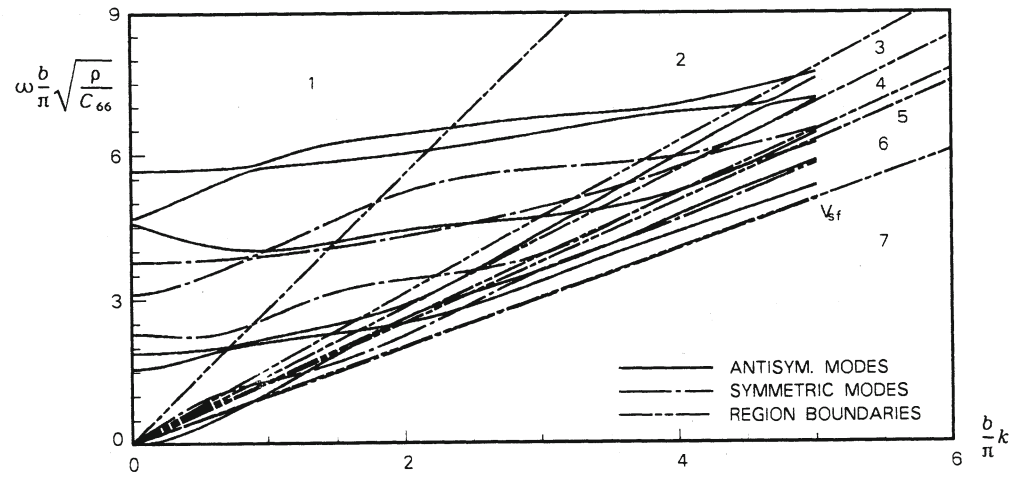

(f)

Fig. 3. Cont'd. (d) Strongly orthotropic ($\alpha = 5°$); (e) Strongly orthotropic ($\alpha = 0$); (f) Strongly orthotropic ($\alpha = 5°$).

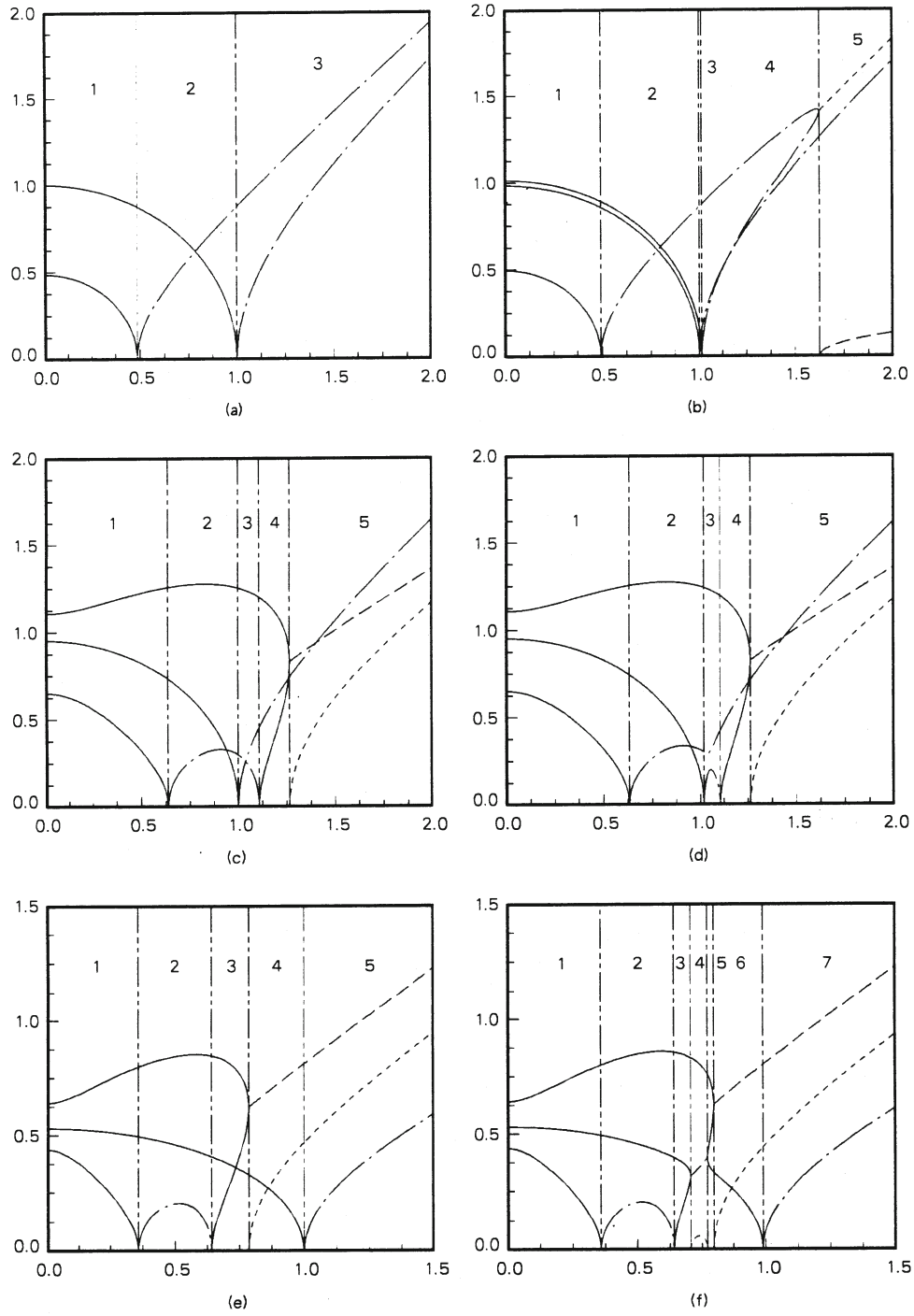

Fig. 4. First quadrant of full plane slowness curves associated with the dispersion curves in Fig. 3. All abscissae are $\frac{k}{\omega}\sqrt{\frac{c_{66}}{\rho}}$ and all ordinates are $\frac{k_3}{\omega}\sqrt{\frac{c_{66}}{\rho}}$. The legend is as following: ——— real; -·- imaginary; — — — — real part of complex; - - - - - imaginary part of complex; -··- region boundaries.

It can be further shown analytically that, when the Rayleigh velocity occurs in the all complex eigenvalue region, there are infinite equally spaced crossings between the S_0 and A_0 modes, and all the crossings fall on the Rayleigh velocity line in the dispersion curves; i.e. the phase velocities of all the A_0 and S_0 mode crossing points are identical and equal to that of Rayleigh wave. This is true even when Rayleigh wave speed is greater than that of SH_0 mode (see Fig. 3 (e)).

For propagation in non-symmetry directions, the SH modes are no longer decoupled. The surface wave then must have imaginary parts in all eigenvalues to ensure the "exponential decay" character. There are two cases: (1) all eigenvalues are pure imaginary, (2) one pair of eigenvalues are pure imaginary and the other two pairs are complex conjugates. The surface wave speed can be determined from $P_1 + P_2 \pm P_3 = 0$, where P_i are as defined earlier. Here, "+" is for case 1 and "-" is for case 2. The plane of particle motion for the surface wave is no longer parallel to the propagation direction. Depending on the anisotropy and propagation angle with respect to symmetry direction, the surface wave may be quasi-SH type (Fig. 3 (f)) or may not be (Fig. 3(d)). When it is quasi-SH type, the A_0 mode in dispersion curves looks nondispersive, resembling the SH_0 mode. This is demonstrated in Fig. 3 (f) where A_0 and the boundary lines separating region 6 and 7 are so close that it is difficult to distinguish them visually. The surface wave is always the asymptote of the A_0 and S_0 modes, although the rate of convergence may differ greatly for different anisotropy. The A_0 and S_0 modes, as they approach the surface velocity, may or may not cross each other. When they do cross, there may be only finite number of crossings. In the case of seemingly infinite crossings, the crossings are no longer equally spaced, and the phase velocities of these crossings are not the same as that of surface wave.

In isotropic dispersion curves (Fig. 3 (a)), there are infinite Lamé modes where SH and Rayleigh-Lamb dispersion curves touch each other tangentially at $\frac{b}{\pi}k = n$. In anisotropic media, these modes do not exist any more. For weak anisotropy, near the points $\frac{b}{\pi}k = n$, symmetric and antisymmetric dispersion curves may split or cross over each other, depending on the anisotropy. This feature has been utilized to characterize texture in polycrystal plates possessing orthotropic symmetry [6].

In this paper, we have presented dispersion equations in analytical or semianalytical forms and analyzed some interesting features for elastic wave propagation in a general orthotropic free plate. More study is necessary to completely understand the dispersive behavior of orthotropic free plates.

ACKNOWLEDGMENTS

Ames Laboratory is operated for the U.S. Department of Energy by Iowa State University under contract No. W-7405-ENG-82. This work was supported by the Director for Energy Research, Office of Basic Energy Sciences.

REFERENCES

1. L. P. Solie, Thesis (1971).
2. L. P. Solie and B. A. Auld, J. Acous. Soc. Amer. 54, 50 (1973).
3. S. A. Markus, et al., Sov. J. Nondes. Testing, 21, 739 (1985).
4. B. A. Auld, Acoustic Fields and Waves in Solids, Vol. 2, 1973.
5. C-T. Lim, and G. W. Farnell, J. Appl. Phys. 39, 4319 (1968).
6. Y. Li and R. B. Thompson, these proceedings.